

Efficiency Comparison of Kernel Interpolation Functions for Investigating Spatial Variability of Temperature in Iran

Majid Javari

College of Social Science, Payame Noor University, IRAN

ABSTRACT

The kernel interpolation techniques provide a suitable spatial format that computes a temperature output layer for temperature output pattern. In this study, the efficiency of kernel interpolation functions for investigating spatial variability of temperature in Iran were studied during 39 years (1975-2014) at 174 stations and 29664 temperature points. In this study, six functions (Exponential, Gaussian, Guartic, Epanechnikov, Polynomial5 and Constant) were used to analyze and forecast monthly, seasonal and annual temperature kernel function patterns variability. Among the kernel functions, the strongest effect was discovered between functions for temperature forecasting the Exponential function at all stations during 39 years. The results showed that the increases in spatial variations of the temperature were occurring mostly in mountainous regions and there are different temperature spatial variation patterns (effect factors) in Iran. In addition, the significant relationships were observed at 174 stations and 29664 points for spatial variations of temperature in Iran.

KEYWORDS

kernel interpolation, spatial variability, functions and Temperature.

ARTICLE HISTORY

Received 20 April 2016
Revised 28 June 2016
Accepted 19 December 2016

Introduction

Temperature is one of the most important elements in climatic analysis. Variability in temperature distribution may lead to economic issues. Temperature variability can significantly affect an environmental process (Bajat et al., 2015). Temperature has changed significantly in different parts of the globe during the recent decades (Benavides et al., 2007). In recent years, Kernel functions have received major attention, particularly due to the increased popularity of the Support Vector Machines (Appelhans et al., 2015). Therefore, the spatial kernel patterns variability of temperature effects are important for climatic analysis and environmental planning. To predict spatial similar variations of temperature, different kernel statistics models have been used

CORRESPONDENCE Majid Javari ✉ majid_javari@yahoo.com

© 2017 M. Javari.

Open Access terms of the Creative Commons Attribution 4.0 International License apply. The license permits unrestricted use, distribution, and reproduction in any medium, on the condition that users give exact credit to the original author(s) and the source, provide a link to the Creative Commons license, and indicate if they made any changes. (<http://creativecommons.org/licenses/by/4.0/>)

(Krivoruchko and Gribov, 2004). Forecasting methods use kernel model outputs for evaluating the impact of temperature changes on the climatic systems, because the spatial formation of kernel statistics models remains quite soft and is suitable for climatic studies (Frączek et al., 2003). The kernel interpolation techniques provide a suitable spatial format that computes a temperature output layer where the value for temperature output pattern is a function of the values of temperature input pattern for any station that falls within a specified similarity to that station location (Hengl, 2009; Juan et al., 2011). The statistical function was performed on the input such as the Exponential, Gaussian, Quartic, Epanechnikov, Polynomial5 and Constant for all temperature values encountered in that kernel models (ESRI, 2014; Johnston et al., 2001). This study relies on a kernel interpolation analysis to measure spatial kernel variability test of monthly temperature, and to estimate temperature distribution by forecasting the kernel interpolation parameters of the distribution as kernel statistical functions. Conceptually, for each station in the output temperature layer, the algorithm determines which of the temperature stations fall within the specified kernel patterns of that cell (Lanfredi et al., 2015). The particular functions selected are applied to the values of the specified field of those temperature stations. The kernel functions can overlap so that stations located in one kernel around the processing cell may also be included in the kernel of another processing cell. The kernel functions are Exponential, Gaussian, Quartic, Epanechnikov, Polynomial5 and Constant. Each function is defined by two parameters, as prediction and prediction standard errors. The paper uses kernel functions to produce perspectives on the variation in monthly temperature over Iran. Kernel functions create temperature output values for each cell station location based on the station value and the values identified in a specifically similar way (Pohlmann, 1993; Stein et al., 1994). The kernel functions calculate temperature output values by calculating a specified statistic to all the temperature station cells that are included in each kernel pattern. The kernel functions analysis of monthly temperature allows to control the cell size and cell alignment of the temperature output layer, as well as to limit the analysis to specific similar way within the analysis extent (Tadić et al., 2015; Wang et al., 2014). The studies on the spatial kernel variability of different regions in Iran are faint in the context of spatial-regional variability in temperature. Low temperature and its severe variations in the monthly spatial scales are the general characteristics of Iran's climates (Alijani et al., 2008; Khalili et al., 2015). Six important indices are Exponential statistics (ES), Gaussian statistics (GS), Quartic statistics (QS), Epanechnikov statistics (EPS), Polynomial5 statistics (PS) and Constant statistics (CS). The ES index is a useful index used in many studies, while other indices have recently been introduced and noticed (ESRI, 2014). The GS and GUS are suitable indices describing and forecasting the temperature spatial distribution mostly used in the monthly time scale (Hengl, 2009). Spatial kernel function patterns variability (SKFPV) of monthly temperature was applied to quantify the significance of magnitude of spatial temperature variations, respectively. Functions commonly used in kernel statistical analysis have been favored over spatial statistical methods. The geo-statistical models have been frequently used

to estimate the significance of spatial variations in temperature series (ESRI, 2014; Javari et al., 2010). The Kernel Interpolation Method (KIM) does not provide an estimate of the magnitude of the spatial variations itself. For this purpose, the other methods referred to as the ES, GS, QS, EPS, PS and CS are very popular by the climatologists to measure the slope of spatial variations. KIM method provides a more powerful deterministic estimate than the other methods because it is suitable to outliers or extreme values (Hengl, 2009; javari, 2015). The objective of this paper is to analyze and forecast the period (1975–2014) of spatial kernel variations of monthly temperature in Iran utilizing 174 station data and 29664 temperature points. The geostatistical model was applied to detect the significant variation; KIM was applied to determine the variation magnitude; and, SKFPV was applied for temperature spatial variations. The analyses and forecasts were conducted for the whole Iran as well as morphological regions of Iran on a seasonal and monthly basis. It is important that the findings of this study will bring about more insights for understanding regional climatic conditions over the last periods in Iran. In final, this paper indicates that little work has been done on the climatology and spatial pattern of monthly and seasonal temperature in Iran.

Materials and methods

Study area and materials

Iran lies between $25^{\circ} 3' - 39^{\circ} 47' N$ in latitude and $44^{\circ} 5' - 63^{\circ} 18' E$ in longitude in the south-western of Asia (Fig. 1). The total area of the Iran is approximately 1,348,195 km². Almost all parts of Iran have four seasons.

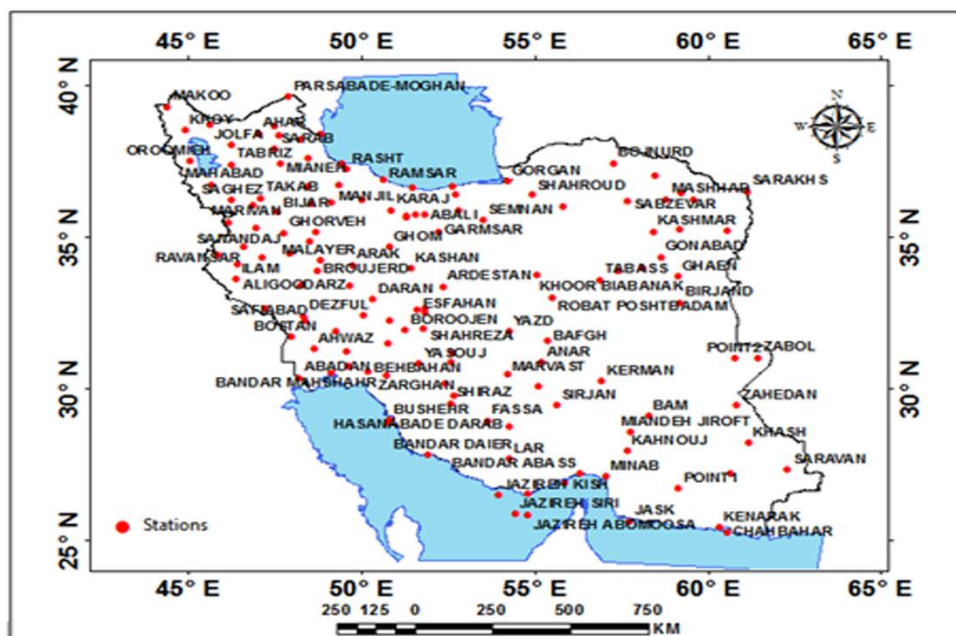


Figure1. Location of stations

The annual rainfall maximum are located on the southwestern of the Khazar Sea, in the northwest on the western slopes of the Zagros Mountains around the Sanandaj and Ravansar meteorological stations, and on the southern slopes of the southern Zagros Mountains around the Baft station (Alijani et al., 2008). The interior parts of the Iran receive much less precipitation. More than half of the Iran receives less than 200mm and some parts get less than 50mm annually. Seasonal Temperature variations related to Iran's subtropical systems position add to this variability. More than half of the annual rain comes in winter from westerly systems carrying Mediterranean Sea moisture (Alijani et al., 2008; Etemadi et al., 2015; Ghajarnia et al., 2015). We were obtained monthly, seasonal and annual Temperature data for all of Iran' 174 stations from the Meteorological Organization of Iran (<http://www.irimo.ir/eng/wd/720-Products-Services.html>) and 29664 Temperature points from has been extracted and processed the Temperature layers of Iran by using ArcGIS(Fig.2). Temperature datasets of 174 stations and 29664 Temperature points across Iran were analyzed for the period of 1975–2014 and autocorrelation analysis were applied to the temperature time series of each station to check the consistency and the homogeneity in the point statistical analysis by using ArcGIS software (<http://www.esri.com>). Fig.2 shows the distribution of 29664 Temperature points in Iran.

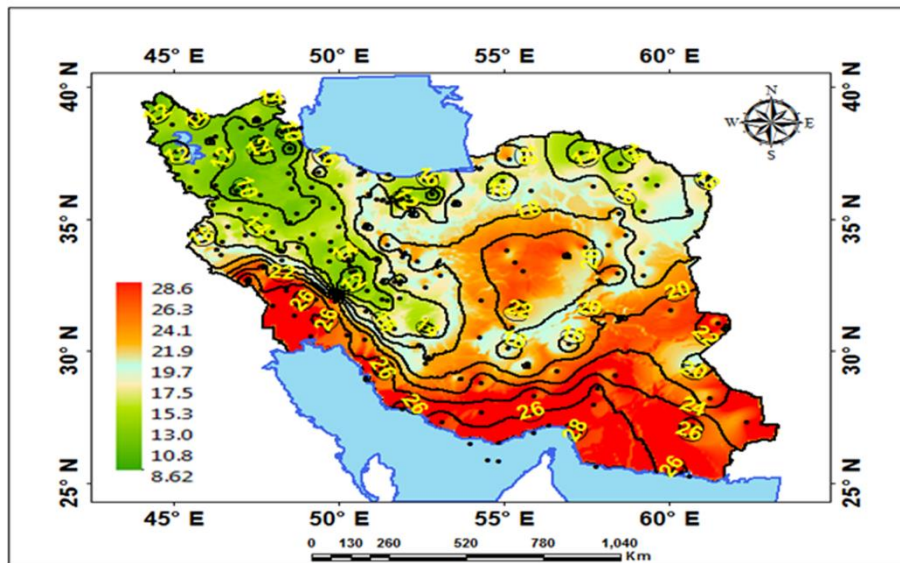


Figure 2. Annual Temperature

In annual scales, highest amount of temperature occur in last 39 years in one of the point situated in Minab station.

Methods

Temperature series of 174 stations and 29664 temperature points have been extracted and studied. The temperature layers have been analyzed using ArcGIS across Iran for the period of 1975–2014. The following methodologies were used in sequence for the analysis; namely: (1) The preliminary drawing

of isotherm of annual temperature series was computed for each station and each temperature point over the period of 1975 to 2014, (2) Series are checked for autocorrelation, (3) Double-mass curve analysis and autocorrelation analysis were applied to the temperature series of each station to check the consistency and the homogeneity. (4) Six important functions including exponential, gaussian, quartic, epanechnikov, polynomial and constant are applied to the whole series to detect the magnitude of the spatial variations, and monthly and seasonal temperature patterns variations. In this study, the exponential function was used to calculate temperature spatial variations pattern at the study stations. The exponential function was presented by the ESRI as a method to estimate temperature spatial variations pattern. The method actuates the temperature as that exponential function is a variant of a first-order Local Polynomial Interpolation in which unsteady in the calculation is arrested using a method similar to the one used in the ridge regression to estimate the regression coefficients. Kernel Interpolation uses the following symmetric kernels: Exponential, Gaussian, Quartic, Epanechnikov, Polynomial of Order 5, and Constant. The bandwidth of the kernel is determined by a rectangle around the observations (ESRI, 2014). With temperature measurements done at 174 stations and 29664 temperature points, the exponential statistics equation is (Johnston et al., 2001; Olea, 2012):

$$ES = e^{-3\left(\frac{R}{H}\right)} \quad (1)$$

Where R = is a radius centered at point *or station* and H is the bandwidth. The bandwidth parameter applies to all kernel functions except Constant. The ArcGIS10.3 software which is able to extract and process the Temperature layers of Iran by using exponential statistics. With temperature measurements done at 174 stations and 29664 temperature points, the Gaussian statistics equation is (Johnston et al., 2001; Oliver and Webster, 2014; Szentimrey et al., 2010):

$$GS = e^{-3\left(\frac{R}{H}\right)^2} \quad (2)$$

According to ESRI (2014) the quartic statistics (QS) can be calculated using the following equation (Johnston et al., 2001):

$$QS = \left(1 - \left(\frac{R}{H}\right)^2\right), \text{ for } \frac{R}{H} < 1 \quad (3)$$

With temperature measurements done at 174 stations and 29664 temperature points, the epanechnikov statistics (EPS) is (Hengl, 2009; Johnston et al., 2001; Oliver and Webster, 2014):

$$EPS = 1 - \left(\frac{R}{H}\right)^2, \text{ for } \frac{R}{H} < 1 \quad (4)$$

According to ESRI (2014) the polynomial statistics (PS) can be calculated using the following equation (Hengl, 2009; Johnston et al., 2001; Oliver and Webster, 2014):

$$PS = 1 - \left(\frac{R}{H}\right)^3 \left(10 - \left(\frac{R}{H}\right) \left(15 - 6 \left(\frac{R}{H}\right)\right)\right), \text{ for } \frac{R}{H} < 1 \quad (5)$$

The constant statistics (CS), is an indicator function that takes a value of 1 if expression is true and a value of 0 if expression is false and it is estimated from the expression (Johnston et al., 2001):

$$CS = I(s - H < s_i < s + H) \quad (6)$$

where I is an indicator function. According to ESRI (2014) the regression coefficients can be calculated using the following equations (Hengl, 2009; Oliver and Webster, 2014):

$$Z = f(x, y) + \varepsilon \quad (7)$$

and the predictions are made by:

$$\hat{Z}(s_0) = \sum_{r, s \in n} \alpha_{rs} \times x^r y^s \quad (8)$$

In this study, the exponential interpolation prediction error is estimated assuming that the model is correct, was used that is the temperature spatial variation pattern is very small. In this study, the predictions and prediction standard errors were forecasted as the validity indices of the RMSE, respectively. According to Neter et al. (1996) the regression errors can be calculated using the following equations (ESRI, 2014; Hengl, 2009; Johnston et al., 2001; Neter, 1996):

$$\varepsilon(s_0) = MSE \times \left[\mathbf{1} - \mathbf{Q}_0^t \times (\mathbf{Q}^t \times \mathbf{Q})^{-1} \times \mathbf{Q}_0 \right] \quad (9)$$

where $Q_k(s_0)$ are the values of the explanatory variables at the target location and MSE is the mean square error around the regression line (Hengl, 2009; Martínez-Cob, 1996; Ozelkan et al., 2015; Wang et al., 2014):

$$MSE = \frac{\sum_{i=1}^n [z(s_i) - \hat{z}(s_i)]^2}{n-2} \quad (10)$$

According to Hwang et al. (2013) the root mean square prediction error (RMSE) and statistical indices are used to forecast the models which are presented below for the measurement of accuracy of the model and efficiency of kernel interpolation functions. For investigating spatial variability of temperature in Iran the following equation can be used. (Halali et al.; Hengl, 2009; Hwang and Choi, 2013; Javari, 2010; Rivero et al., 2007):

$$R^2 = \left(\frac{\sum (x_i - \bar{x})(y_i - \bar{y})}{\sqrt{\sum_i (x_i - \bar{x})^2 \sum_i (y_i - \bar{y})^2}} \right)^2 \quad (11)$$

$$RMSE = \sqrt{\frac{\sum_{i=1}^n [z(s_i) - \hat{z}(s_i)]^2}{n-2}} \quad (12)$$

R^2 is coefficient of determination that is simply the square of the correlation coefficient. SS_T is sum of squared prediction and SS_E is sum of squared residuals. The amounts of RMSE at each station and at each month were then compared statistically to other functions of the month by a validity index. Validity indices of the results are based on the amounts of RMSE between

the monthly temperature values corresponding to the various functions for the entire period (1975-2014). In addition, exponential, Gaussian, and constant kernel functions additionally support a smooth searching neighborhood in order to limit the range of the kernel. The standard search neighborhood is defined by the ellipse parameters: angle, major semiaxis, and minor semiaxis (ESRI, 2014). A kernel smoother obtains a fitted value by taking a weighted average of the temperature series, with the weight decreasing for points further from the location of interest. Kernel smoothers are classical smoothers that are less sophisticated than the other smoothers available. In addition to the smoothing factor, the variations between the temperature values and the exponential, Gaussian and constant functions with 0.2 coefficient were analyzed during the entire period.

Results and discussion

In this study, six different functions as kernel functions were used to analyze and forecast monthly, seasonal and annual temperature patterns variability. Fig.2 shows the temperature variations in 29664 annual temperature points respectively at 174 stations during 1975–2014. In this paper, the temperature patterns variations concerning the kernel functions were considered for the monthly, seasonal and annual temperature at the 174 stations and 29664 temperature points. The variations of temperature cross validation (1975–2014) sandwiched between the kernel functions for the temperature are shown in Fig. 3.



Figure 3. The variations of temperature cross validation (1975–2014) sandwiched between the kernel functions for the temperature

As shown in Table.1, the R^2 of the kernel functions for the monthly, seasonal and annual temperature were neighboring. In fact, maximum ($R^2 = 0.987$) and minimum ($R^2 = 0.559$) of the kernel functions were respectively significant during the period. The results also showed that all of the R^2 of the kernel functions between the monthly, seasonal and annual period were acceptable at January (0.987) and August (0.559).

Table 1. Amounts of R^2 at each methods

Function Temperature	Exponential	Gaussian	Quartic	Epanechnikov	Polynomial5	Constant
	R^2	R^2	R^2	R^2	R^2	R^2
Winter	0.972	0.812	0.742	0.712	0.872	0.752
Spring	0.921	0.761	0.691	0.661	0.821	0.701
Summer	0.841	0.681	0.611	0.581	0.741	0.621
Autumn	0.965	0.805	0.735	0.705	0.865	0.745
January	<u>0.987</u>	0.827	0.757	0.727	0.887	0.767
February	0.982	0.822	0.752	0.722	0.882	0.762
March	0.965	0.805	0.735	0.705	0.865	0.745
April	0.946	0.786	0.716	0.686	0.846	0.726
May	0.934	0.774	0.704	0.674	0.834	0.714
June	0.873	0.713	0.643	0.613	0.773	0.653
July	0.826	0.666	0.596	0.566	0.726	0.606
August	0.819	0.659	0.589	<u>0.559</u>	0.719	0.599
September	0.874	0.714	0.644	0.614	0.774	0.654
October	0.932	0.772	0.702	0.672	0.832	0.712
November	0.969	0.809	0.739	0.709	0.869	0.749
December	0.985	0.825	0.755	0.725	0.885	0.765
Annual	0.937	0.777	0.707	0.677	0.837	0.717

As shown in Table.2, the RMSE of the kernel functions for the monthly, seasonal and annual temperature was contiguous.

Table 2. Amounts of RMSE at each methods

Function Temperature	Exponential	Gaussian	Quartic	Epanechnikov	Polynomial5	Constant	Selected kernel function
	RMSE	RMSE	RMSE	RMSE	RMSE	RMSE	Least of RMSE
Winter	2.05	2.151	2.089	2.141	2.071	2.22	Exponential

Spring	2.32	2.43	2.37	2.42	2.36	2.505	Exponential
Summer	2.32	2.407	2.36	2.40	2.353	2.473	Exponential
Autumn	2.067	2.159	2.097	2.153	2.076	2.226	Exponential
January	2.08	2.178	2.117	2.17	2.095	2.248	Exponential
February	2.141	2.303	2.139	2.193	2.14	2.279	Quartic
March	2.099	2.169	2.1	2.158	2.09	2.24	Polynomial5
April	2.198	2.281	2.21	2.27	2.172	2.36	Polynomial5
May	2.37	2.484	2.43	2.48	2.418	2.561	Exponential
June	2.596	2.591	2.597	2.598	2.599	2.663	Gaussian
July	2.379	2.462	2.415	2.453	2.416	2.527	Exponential
August	2.365	2.453	2.403	2.445	2.399	2.519	Exponential
September	2.364	2.367	2.375	2.363	2.386	2.43	Epanechnikov
October	2.217	2.312	2.59	2.31	2.24	2.376	Exponential
November	2.06	2.16	2.09	2.15	2.07	2.23	Exponential
December	2.01	2.09	2.025	2.08	2	2.154	Polynomial5
Annual	2.133	2.23	2.173	2.222	2.16	2.30	Exponential

In fact, about 0.663 (2 to 2.663) of the continuous range respectively in all period was insignificant. The results also showed that all of the RMSE of the kernel functions concerning the temperature at December (2) and June (2.663) were inappreciable. The RMSE assessed the relationship between the kernel functions for the temperature in Iran. The RMSE establish very strong relationships between the kernel patterns variations for temperature in Iran. The RMSE considered the important role played by temperature for spatial patterns variations forecast of temperature and selection of kernel functions type for analysis of temperature in Iran. The results for the selected kernel functions type of the temperature at the study stations were summarized in Table 2. The kernel functions for the variations of the temperature were eleven exponential methods for monthly, seasonal and annual series. In this study, the exponential prevalent pattern of kernel at the seasonal and annual temperature variability was forecasted during 39 years (1975-2014) at 174 Iran stations and 29664 temperature points. The results showed that the temperature seasonal variations frequently were predictable with the exponential spatial patterns at all of the stations. To compare the kernel functions, the difference between the temperature spatial patterns variations during the months were also categorized at all stations. The results of the differences between the temperature spatial patterns variations during the months are shown in Figs.4–15. Fig. 4 shows the spatial variations of the January temperature by exponential function of kernel.

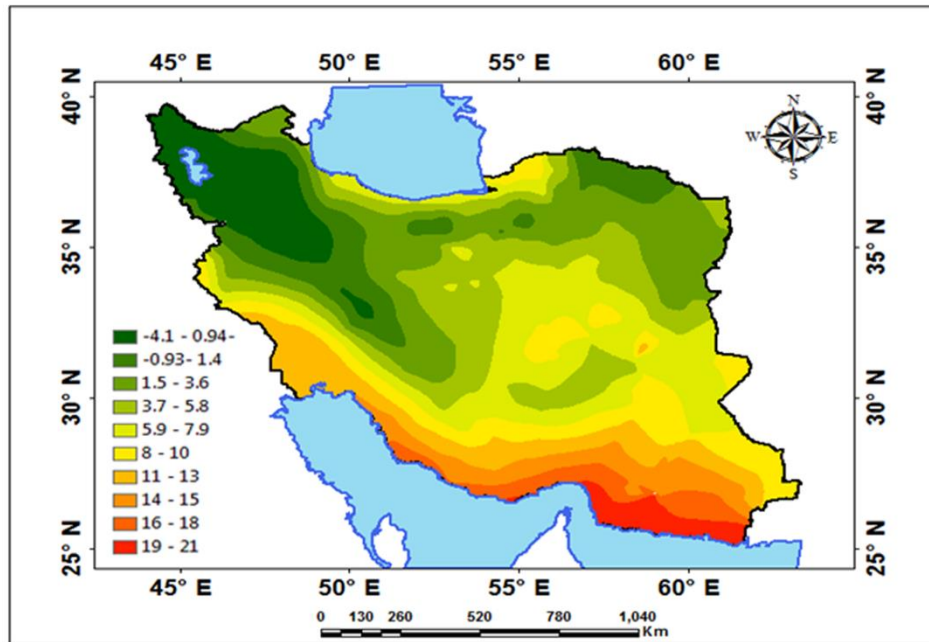


Figure 4. January Temperature Prediction with Exponential Function

The variations range of the January temperature with exponential function in the stations was detected in 25.1 °C, primarily. This indicates the stronger spatial variations of temperature during January in mountain zones of western north and west in Iran. In addition, this indicates the stronger effects of mountain on temperature variability during January in north than south parts and at this month, the temperature variability values were from northwest to southeast higher than the temperature variability values. Fig. 5 shows the spatial variations of the February temperature by Quartic function of kernel. The variations range of the January temperature with Quartic function in the stations was examined in 22.8 °C, mainly.

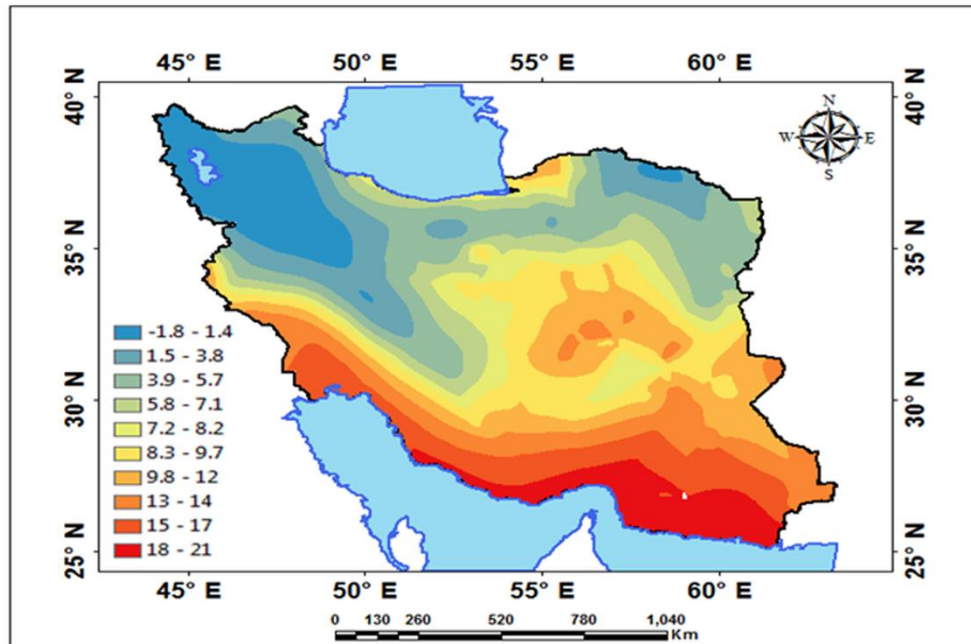


Figure 5. February Temperature Prediction with Quartic Function

This indicates the weaker spatial variations of temperature during February in mountainous zones of northwest and west in comparison to January in Iran. Forecast of the spatial distribution of the temperature variability values during January and February demonstrated that most of the significant temperature variability occurred in the southeastern and southern regions of Iran. Fig. 6 shows the spatial variations of the March temperature by polynomial5 function of kernel.

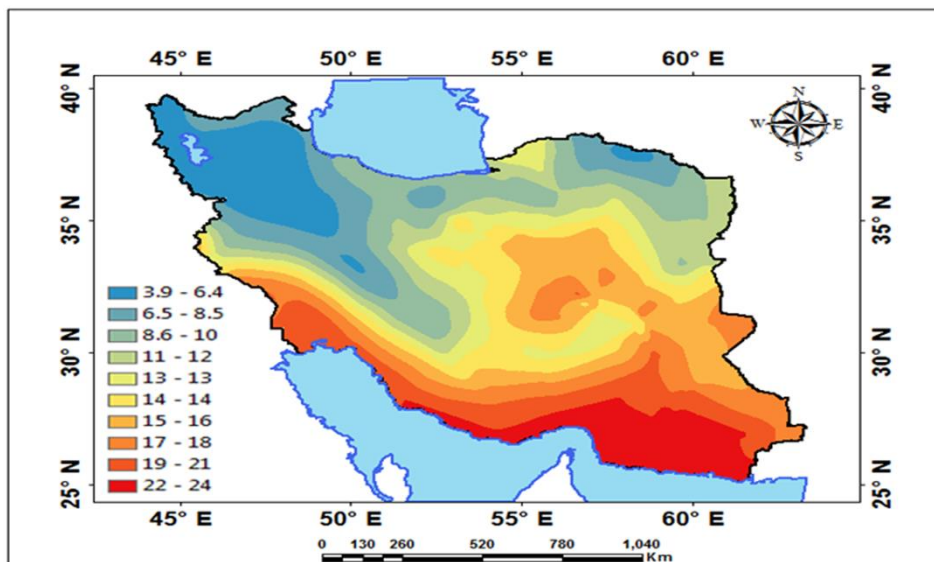


Figure 6. March Temperature Prediction with polynomial5 Function

The variations range of the January temperature with Quartic function in the stations was seen in $20.1\text{ }^{\circ}\text{C}$, frequently. This designates the weaker spatial variations of temperature during March than January and February in Iran. Forecast of the spatial distribution of the temperature variability values during March demonstrated that the lowest of the significant temperature variability occurred in the center and central regions of Iran. Fig. 7 displays the spatial variations of the April temperature by Exponential function of kernel.

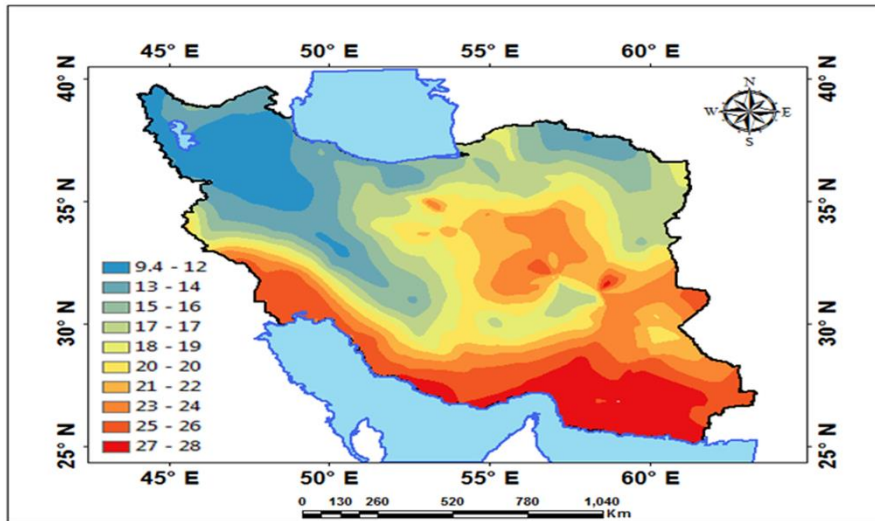


Figure 7. April Temperature Prediction with Exponential Function

The variations range of the April temperature with Exponential function in the stations was surveyed in $18.6\text{ }^{\circ}\text{C}$, normally. This denotes the weaker spatial variations of temperature during April than previous months in Iran. Forecast of the spatial distribution of the temperature variability values during April determined that the lowest of the significant temperature variability appeared in the northwest of Iran. Fig. 8 shows the spatial variations of temperature in May by Exponential function of kernel.

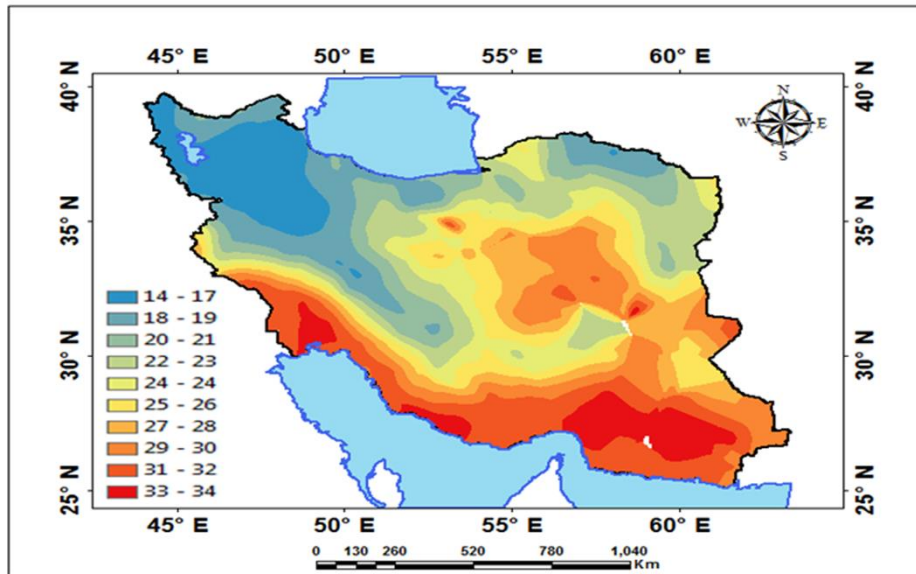


Figure 8. May Temperature Prediction with Exponential Function

The variations range of the April temperature with Exponential function in the stations was reflected in 20 °C, repeatedly. This shows the stronger spatial variations of temperature during May than April in Iran. Prediction of the spatial scattering of the temperature variability values during May established that the lowest of the significant temperature variability happened in the western north of Iran and highest of the significant temperature variability appeared in the southeast of Iran. Fig. 9 illustrates the spatial variations of the June temperature by Gaussian function of kernel.

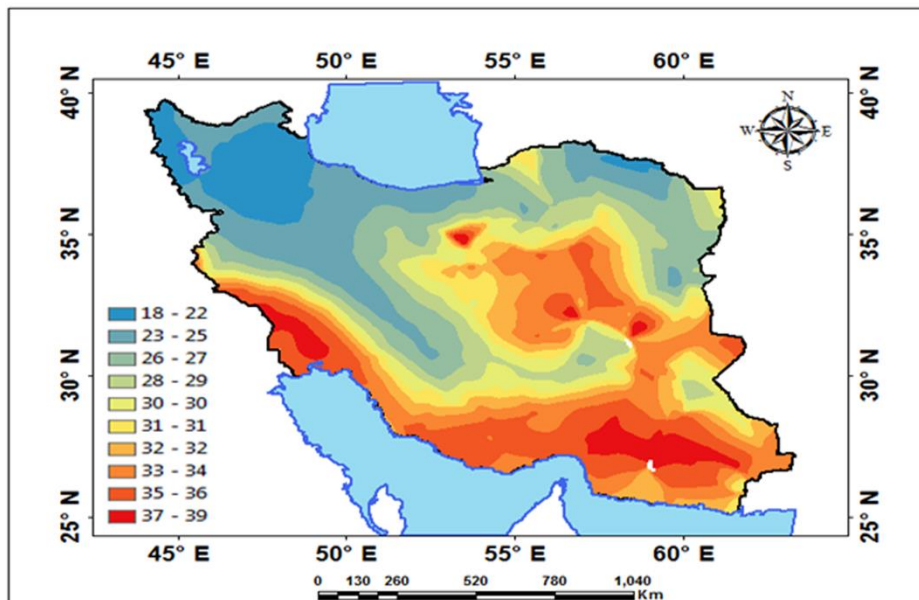


Figure 9. June Temperature Prediction with Gaussian Function

The variations range of the June temperature with Gaussian function in the stations was viewed in 21 °C, commonly. During the June (Fig. 9), the spatial variations of the temperature increased to 39 °C representing that the occurrence of the multiplier factors generally led to an increase in the June temperature in Iran. Similar to the May temperature pattern, the highest of the spatial variations of temperature appears in the south and eastern half of Iran. Fig. 10 demonstrates the spatial variations of the July temperature by Exponential function of kernel.

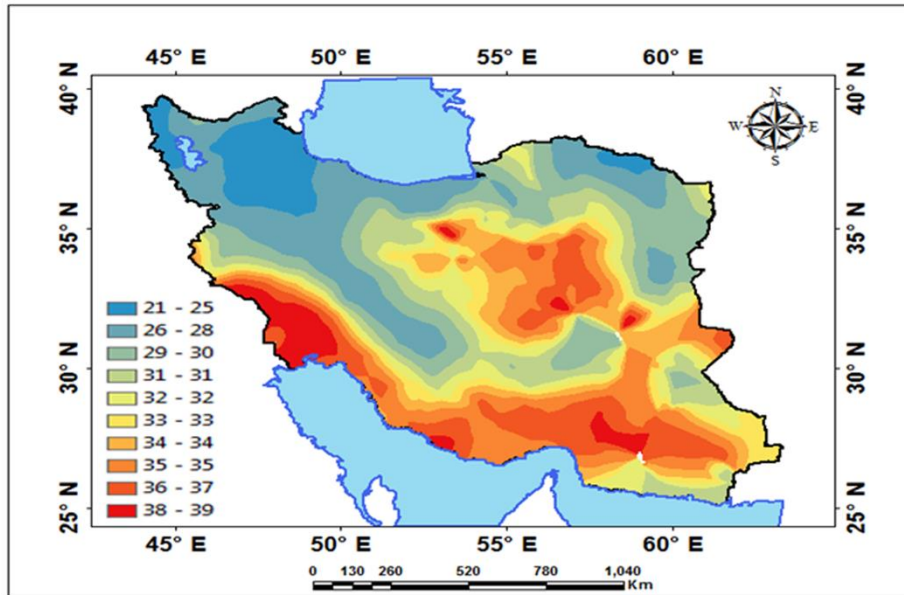


Figure 10. July Temperature Prediction with Exponential Function

The variations range of the July temperature with Exponential function in the stations was observed in 18 °C, frequently. During the July (Fig. 10), the spatial variations of the temperature increased to 39 °C in Iran. Forecast of the spatial distribution of the temperature variability values during July established that the lowest of the significant temperature variability occurred in the northern half of Iran and the highest of the significant temperature variability in the southern half of Iran. Fig. 11 shows the spatial variations of the August temperature by Exponential function of kernel.

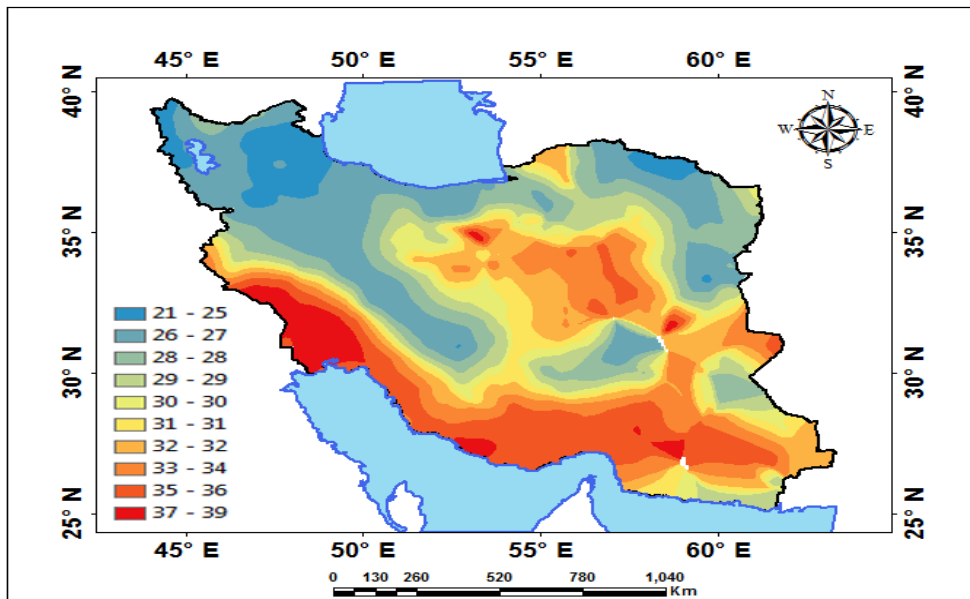


Figure 11. August Temperature Prediction with Exponential Function

The variations range of the July temperature with Exponential function in the stations was detected in 18 °C, frequently. Similar to the July temperature pattern, the highest of the spatial variations of temperature appears in August in the southern half of Iran. Fig. 12 shows the spatial variations of the September temperature by Epanechnikov function of kernel. The variations range of the September temperature with Epanechnikov function in the stations was declared in 16 °C, repeatedly. During the September (Fig. 12), the spatial variations of the temperature decreased to 34 °C in Iran.

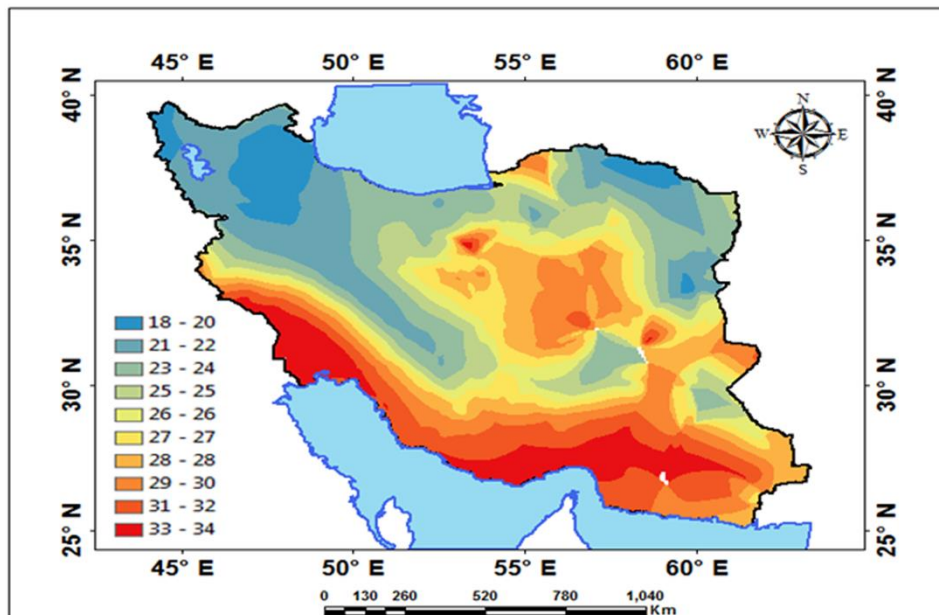


Figure 12. September Temperature Prediction with Epanechnikov Function

Similar to the August temperature pattern, the highest of the spatial variations of temperature appears in September in the southern half and southwest of Iran. Fig. 13 indicates the spatial variations of the October temperature by Exponential function of kernel.

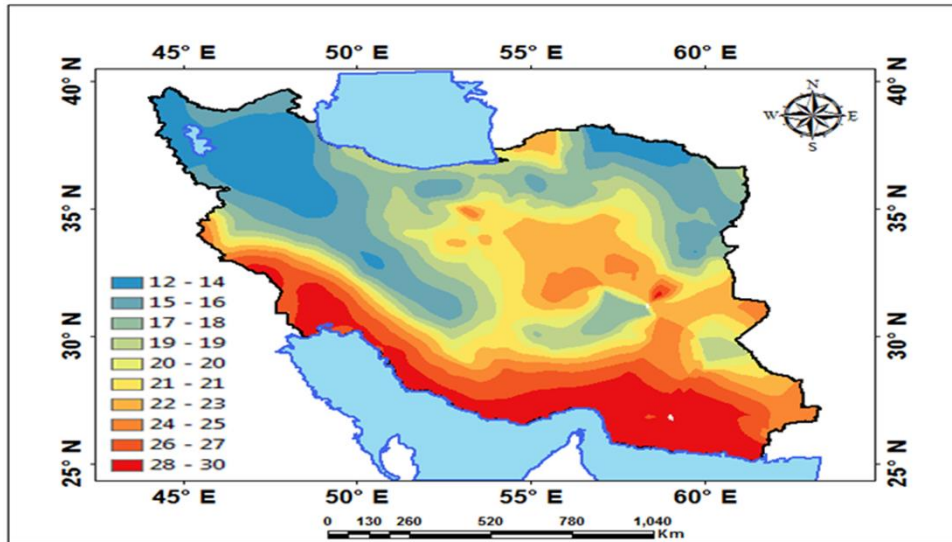


Figure 13. October Temperature Prediction with Exponential Function

The variations range of the October temperature with Exponential function in the stations was remarked in 18 °C, frequently. Similar to the September, the highest of the spatial variations of temperature occurs in October in the southern half and southwest of Iran. Fig. 14 displays the spatial variations of the November temperature by Exponential function of kernel.

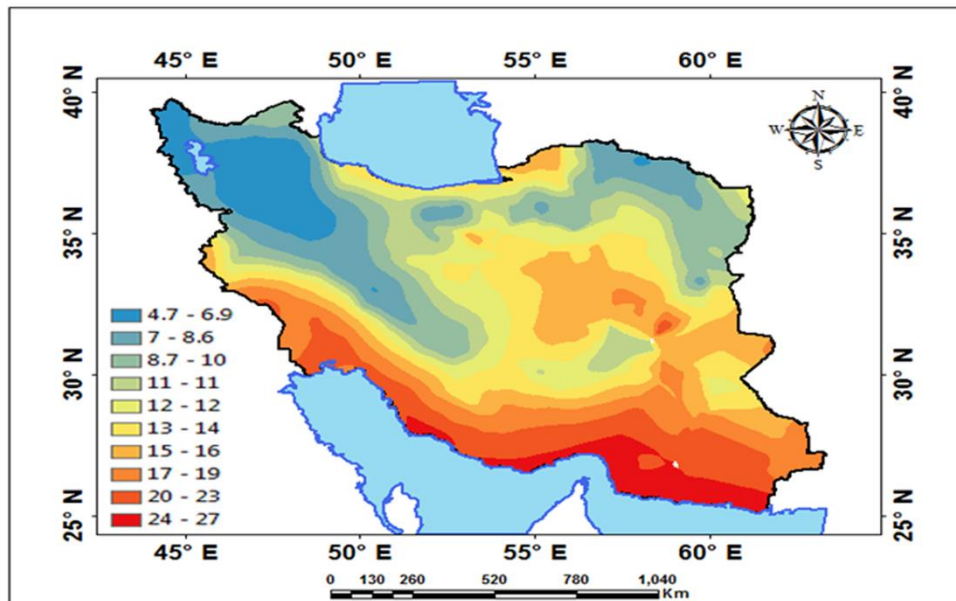


Figure 14. November Temperature Prediction with Exponential Function

The variations range of the November temperature with Exponential function in the stations was observed in 22.3 °C, commonly. During the November (Fig. 14), the spatial variations range of the temperature increased to 22.3 °C in Iran. Similar to the October, the highest of the spatial variations of temperature seems in November in the southern half and southwest of Iran. Fig. 15 shows the spatial variations of the December temperature by polynomial5 function of kernel. The variations range of the December temperature with polynomial5 function in the stations was viewed in 24.2 °C, normally. Similar to the November, the highest of the spatial variations of temperature appears in December in the southern half and southwest of Iran.

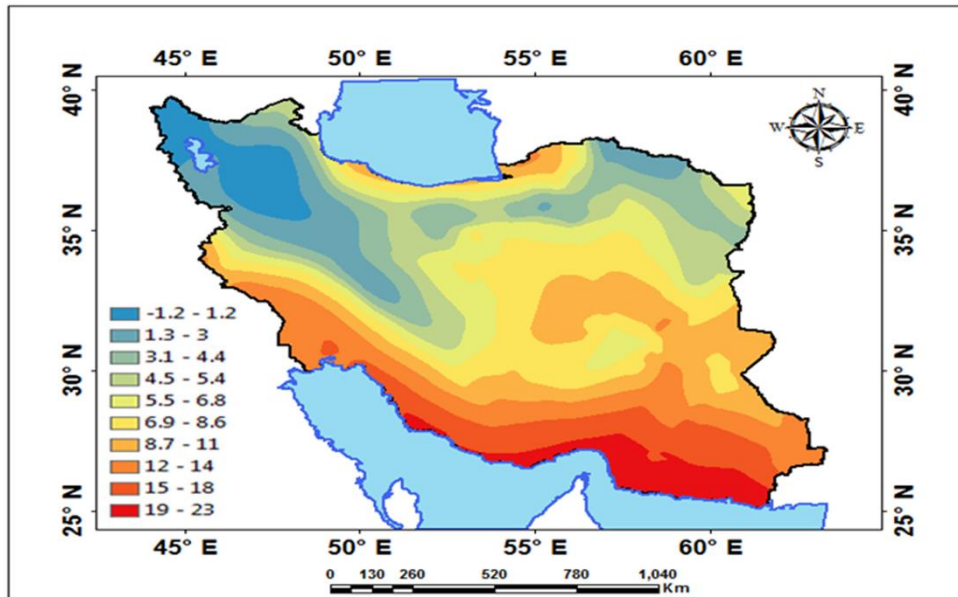


Figure 16. December Temperature Prediction with polynomial5 Function

Fig. 16 displays the spatial variations of the winter temperature by Exponential function of kernel. The variations range of the winter temperature with Exponential function in the stations was seen in 22.75°C , frequently. As shown in Fig. 16, the spatial variations of the winter temperature were different between northern and southern halves. During the winter (Fig. 16), the spatial variations range of the temperature at southern half increased to 12°C in Iran.

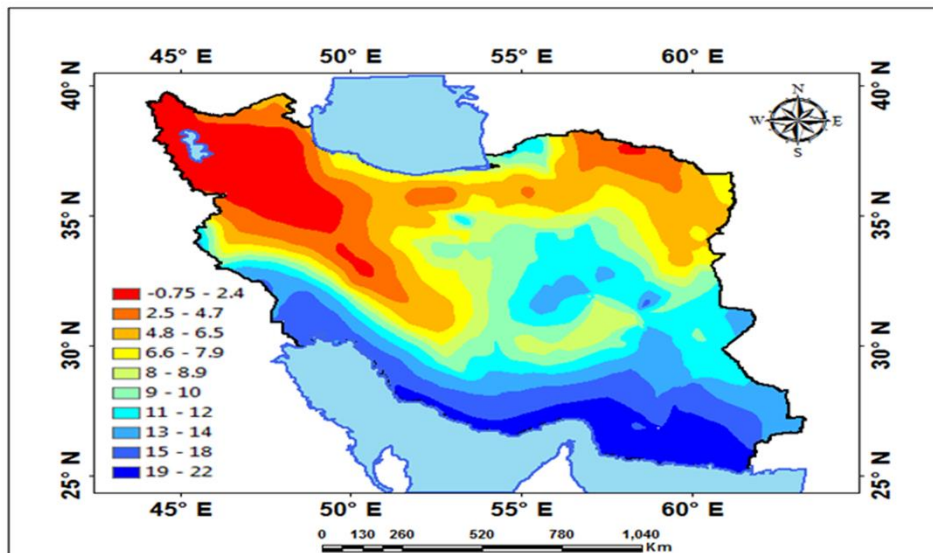


Figure 16. Winter Temperature Prediction with Exponential Function

Fig. 17 shows the spatial variations of the spring temperature by Exponential function of kernel. The variations range of the spring temperature

with Exponential function in the stations was perceived in 19 °C, frequently. As revealed in Fig. 17, the spatial variations of the spring temperature were different between northern and southern halves. During the spring (Fig. 17), the spatial variations range of the temperature at northern half increased to 9 °C in Iran.

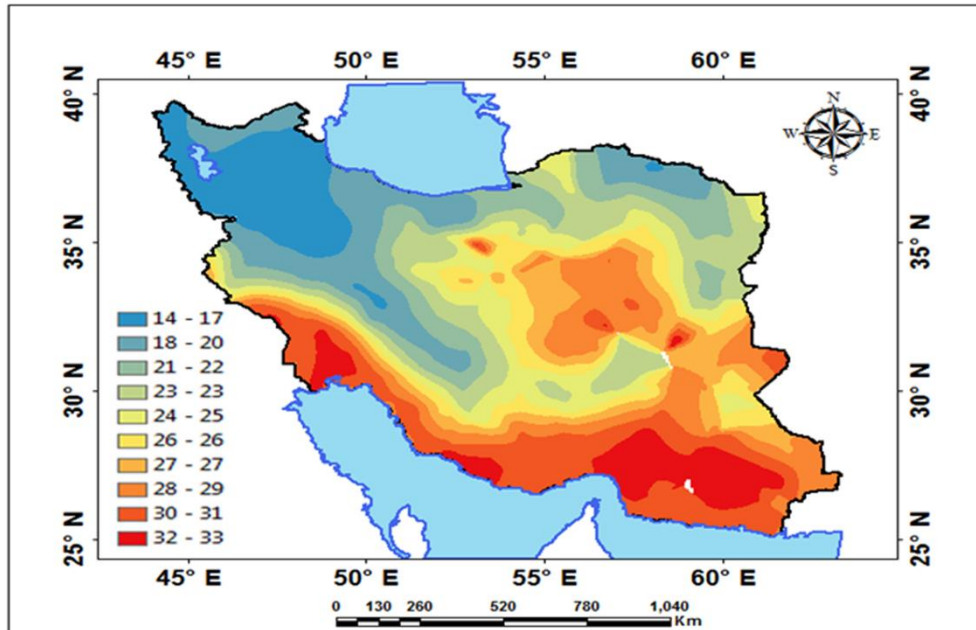


Figure 17. Spring Temperature Prediction with Exponential Function

Fig. 18 shows the spatial variations of the summer temperature by Exponential function of kernel. The variations range of the summer temperature with Exponential function in the stations was recognized in 18 °C, frequently. As presented in Fig. 18, the spatial variations of the summer temperature were different between northern and southern halves. During the summer (Fig. 18), the spatial variations range of the temperature at northern half than southern half increased to 8 °C in the Iran.

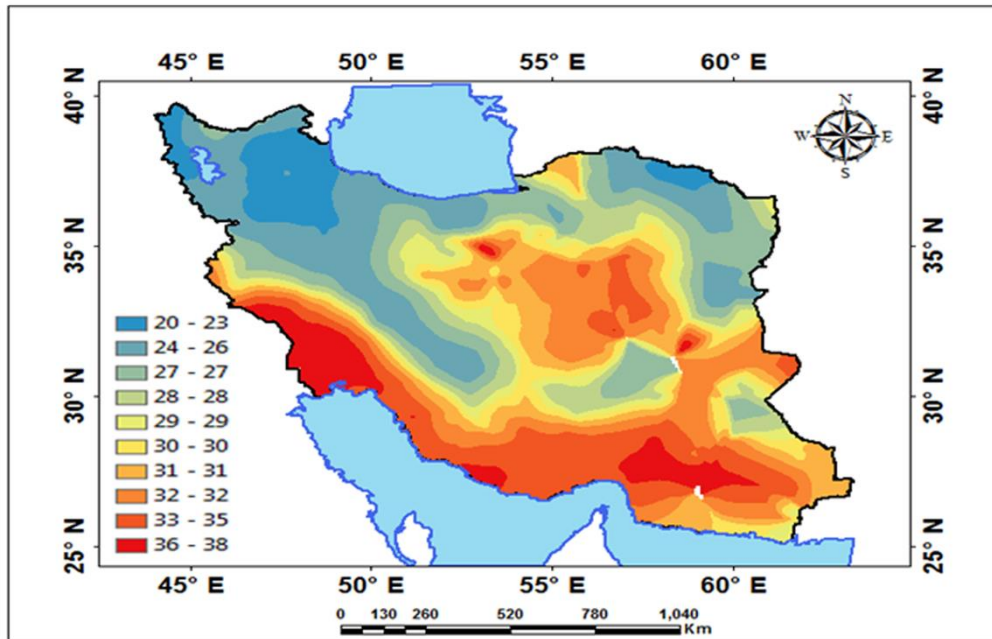


Figure18. Summer Temperature Prediction with Exponential Function

Fig. 19 displays the spatial variations of the autumn temperature by Exponential function of kernel. The variations range of the autumn temperature with Exponential function in the stations was identified in 21.6 °C, frequently. As shown in Fig. 19, the spatial variations of the autumn temperature were diverse between northern and southern halves. During the autumn (Fig. 19), the spatial variations range of the temperature at southern half rather than northern half increased to 13 °C in Iran.

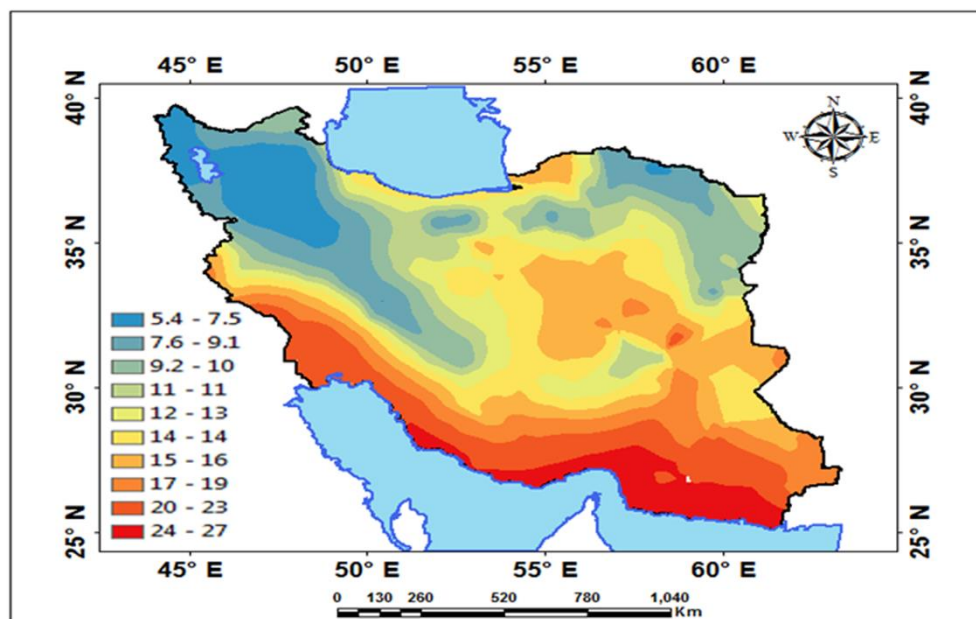


Figure 19. Autumn Temperature Prediction with Exponential Function

The results also showed that the highest spatial variations of temperature happened during the autumn (Fig. 19) in Iran. Fig. 20 appearances the spatial variations of the annual temperature by Exponential function of kernel. The variations range of the annual temperature with Exponential function the in the stations was examined in 18 °C, frequently. As illustrated in Fig. 20, the spatial variations of the annual temperature were approximately similar between northern and southern halves. The results also showed that during the year (Fig. 20), the spatial variations of the temperature occurred uniformly in Iran. Finally, the consequences of the present paper assemble findings for better recognition of the temperature variability in Iran. We originate that the increases in spatial variations of the temperature were occurring mostly in mountain regions and there are different temperature spatial variations patterns (effect factors) in Iran.

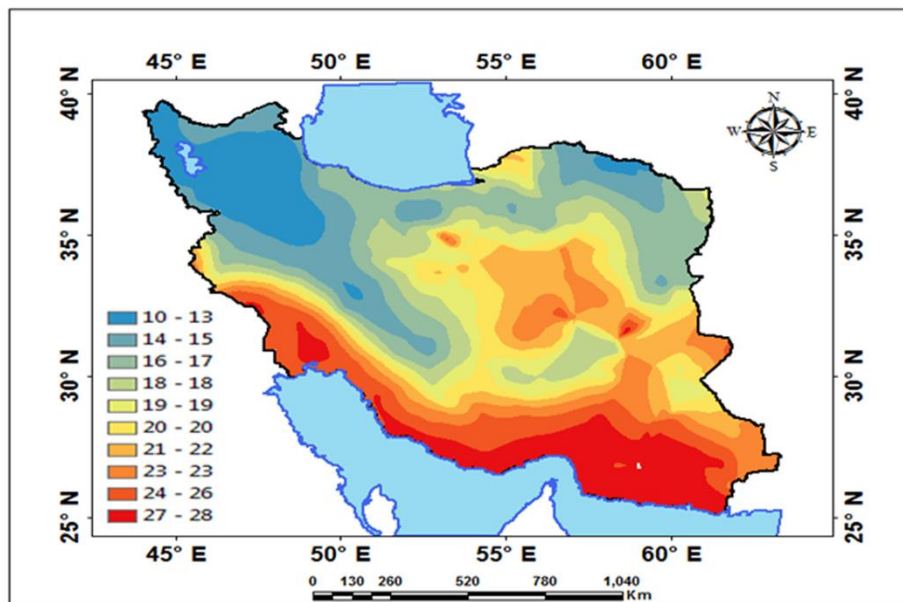


Figure 20. Annual Temperature Prediction with Exponential Function

Therefore, further studies are required revaluing the impacts of the factors variability in Iran.

Conclusions

In this study, the efficiency of kernel interpolation functions for investigating spatial variability of temperature in Iran was studied during 39 years (1975-2014). The results showed that the spatial variability of the monthly, seasonal and annual temperature were various in Iran especially the mountains. Among the kernel functions, the strongest effect was found between functions for temperature forecasting the Exponential function at all stations during 39 years. Of the studied series , monthly , seasonal and annual temperature presented different patterns. At the mentioned functions, the

predominance of the Exponential function between the series was dominant. In addition, the significant relationships were observed at 174 stations and 29664 points for spatial variations of temperature in Iran. We found that the increases in spatial variations of the temperature were occurring mostly in mountainous regions and there are different temperature spatial variations patterns (effect factors) in Iran. Finally, the findings of the present research provide more insights for better recognition of the effects of the kernel functions on the temperature variability Iran. More proceedings are needed to recognize the effects of the large spatial patterns on environmental planning for major economic scopes.

Disclosure statement

No potential conflict of interest was reported by the authors.

Notes on contributors

Majid Javari - Assistant Prof. of Climatology, College of Social Science, Payame Noor University, PO BOX 19395-3697, Tehran, Iran.

References

- Alijani, B., O'Brien, J. and Yarnal, B., 2008. Spatial analysis of precipitation intensity and concentration in Iran. *Theor Appl Climatol*, 94(1-2), 107-124.
- Appelhans, T., Mwangomo, E., Hardy, D.R., Hemp, A. and Nauss, T., 2015. Evaluating machine learning approaches for the interpolation of monthly air temperature at Mt. Kilimanjaro, Tanzania. *Spatial Statistics*.
- Bajat, B., Blagojević, D., Kilibarda, M., Luković, J. and Tošić, I., 2015. Spatial analysis of the temperature trends in Serbia during the period 1961–2010. *Theor Appl Climatol*, 121(1-2), 289-301.
- Benavides, R., Montes, F., Rubio, A. and Osoro, K., 2007. Geostatistical modelling of air temperature in a mountainous region of Northern Spain. *Agricultural and Forest Meteorology*, 146(3–4), 173-188.
- ESRI, 2014. *Spatial Statistics Tools, ArcGIS geostatistical analyst, ArcMap 10.3*. ESRI, Redlands, California. ESRI, ArcMap 10.3. ESRI, Redlands, California.
- Frączek, W., Bytnerowicz, A. and Arbaugh, M.J., 2003. Use of geostatistics to estimate surface ozone patterns. In: M.J.A.R.A. Andrzej Bytnerowicz (Editor), *Developments in Environmental Science*. Elsevier, pp. 215-247.
- Ghajarnia, N., Liaghat, A. and Daneshkar Arasteh, P., 2015. Comparison and evaluation of high resolution precipitation estimation products in Urmia Basin-Iran. *Atmospheric Research*, 158–159, 50-65.
- Halali, M.A., Azari, V., Arabloo, M., Mohammadi, A.H. and Bahadori, A., Application of a radial basis function neural network to estimate pressure gradient in water–oil pipelines. *Journal of the Taiwan Institute of Chemical Engineers*.
- Hengl, T., 2009. *A Practical Guide to Geostatistical Mapping*. Office for Official Publications of the European Communities, Luxembourg.
- Hwang, K. and Choi, M., 2013. Seasonal trends of satellite-based evapotranspiration algorithms over a complex ecosystem in East Asia. *Remote Sensing of Environment*, 137(0), 244-263.
- Javari, M., 2010. *Quantitative Methods in Climatology (Trend Models)*. Payam Resan Press: 30-70.
- Javari, m., 2015. Geostatistical and Spatial Statistical Modelling of Precipitation Variations in Iran. *Journal of Civil & Environmental Engineering*.

- Johnston, K., Ver Hoef, J.M., Krivoruchko, K. and Lucas, N., 2001. Using ArcGIS geostatistical analyst, 380. Esri Redlands.
- Juan, P. et al., 2011. Geostatistical methods to identify and map spatial variations of soil salinity. *Journal of Geochemical Exploration*, 108(1), 62-72.
- Khalili, K., Tahoudi, M., Mirabbasi, R. and Ahmadi, F., 2015. Investigation of spatial and temporal variability of precipitation in Iran over the last half century. *Stoch Environ Res Risk Assess*: 1-17.
- Krivoruchko, K. and Gribov, A., 2004. Geostatistical Interpolation and Simulation in the Presence of Barriers. In: X. Sanchez-Vila, J. Carrera and J. Gómez-Hernández (Editors), *geoENV IV — Geostatistics for Environmental Applications. Quantitative Geology and Geostatistics*. Springer Netherlands, pp. 331-342.
- Lanfredi, M. et al., 2015. A geostatistics-assisted approach to the deterministic approximation of climate data. *Environmental Modelling & Software*, 66(0), 69-77.
- Martínez-Cob, A., 1996. Multivariate geostatistical analysis of evapotranspiration and precipitation in mountainous terrain. *Journal of Hydrology*, 174(1-2), 19-35.
- Neter, J., Kutner, M. H., Nachtsheim, C. J., Wasserman, W. , 1996. *Applied Linear Statistical Models*,. McGraw- Hill, .
- Olea, R.A., 2012. *Geostatistics for engineers and earth scientists*. Springer Science & Business Media.
- Oliver, M.A. and Webster, R., 2014. A tutorial guide to geostatistics: Computing and modelling variograms and kriging. *CATENA*, 113(0), 56-69.
- Pohlmann, H., 1993. Geostatistical modelling of environmental data. *CATENA*, 20(1-2), 191-198.
- Rivero, R.G., Grunwald, S. and Bruland, G.L., 2007. Incorporation of spectral data into multivariate geostatistical models to map soil phosphorus variability in a Florida wetland. *Geoderma*, 140(4), 428-443.
- Stein, A. et al., 1994. A geostatistical analysis of the spatio-temporal development of downy mildew epidemics in cabbage. *Phytopathology*, 84(10), 1227-1239.
- Szentimrey, T., Bihari, Z. and Szalai, S., 2010. Comparison of Geostatistical and Meteorological Interpolation Methods (What is What?), *Spatial Interpolation for Climate Data*. ISTE, pp. 45-56.
- Tadić, J.M., Ilić, V. and Biraud, S., 2015. Examination of geostatistical and machine-learning techniques as interpolators in anisotropic atmospheric environments. *Atmospheric Environment*, 111(0), 28-38.
- Wang, S. et al., 2014. Comparison of interpolation methods for estimating spatial distribution of precipitation in Ontario, Canada. *International Journal of Climatology*, 34(14): 3745-3751.